

# Performance Improvement of AC/DC Matrix Converter with Unbalanced Grid Voltage

N. Rajeswaran<sup>1</sup>, P. Marimuthu<sup>2</sup> and Ilapuram Mahesh<sup>3</sup>

<sup>1,2</sup>Professor, Dept. of Electrical and Electronics Engineering, Malla Reddy Engineering College(A), Secunderabad, Telangana, India 500100

<sup>3</sup>PG Scholar, Dept. of Electrical and Electronics Engineering, Malla Reddy Engineering College (A), Secunderabad, Telangana, India 500100

\*\*\*

**Abstract** - The severe grid current harmonics and ripples on the DC side is induced by means of AC/DC Matrix Converter (MC). The enhanced control tactic for an AC/DC matrix converter is projected to overcome these problems, and based on an independent control proposal for the reactive and active powers. The constant DC voltage, sinusoidal grid current and current are premeditated from the current reference generated is synthesized directly by instant analysis of power in a stationary frame. Because of reactive power control in the grid, the input power factor is approximately unity under the unbalanced conditions. The positive and negative sequences components of grid voltage are no need to extract. Hence, without a large storage requirement the planned control technique can be implemented without any difficulty. The Simulation results are obtained is to verify the efficacy of the proposed control strategy.

**Key Words:** Matrix Converter, vehicle - to - grid, Space Vector Modulation and Voltage Source Converters, Reactive Power Control.

## 1. INTRODUCTION

The various emerging applications, the bidirectional components of AC/DC converter are a vital part, such as storage of energy systems [1], the hybrid AC/DC micro grids [2], and Vehicle - to - Grid (V2G) systems [3]. The voltage source converters are generally used, which have merits of sinusoidal grid current, flow of power in bidirectional, capability of fixed DC voltage regulation and controllable of power factor. But the DC voltage should be larger than the peak value of AC voltage is the intrinsic restraint of VSCs. In general the DC voltage is usually lower than the peak value of AC voltage and might be different over an extensive range for many applications. As a result, the increases of cost and weight while the efficiency of the converter system is reduced by adding the bidirectional component of DC/DC converters to equivalent the preferred DC bus voltage in [4], [5]. In addition, because of the massive capacitor across the DC bus, the power density and reliability of the VSCs are very poor were presented in [6]. The proposed system has lots of advantages such as long life, compact design, controllable power factor and, sinusoidal grid current were presented in [7, 8]. Thus, the AC/DC matrix converter is an elegant option to VSC based topologies for applications with slight DC voltage were presented in [9, 10]. A lot of control schemes

for grid voltage with balanced condition have been offered to effectively operate the AC/DC matrix converter in [10]–[16]. According to the range of output, the proper selection of active vectors are needed in Space Vector Modulation (SVM), in order to trim down the ripples in the output current described in [10], and optimally utilized by the zero vectors. The switching commutation failures and grid current distortion can be eliminated with narrow pulse by the modified SVM were presented in [12], and power factor of the input can be controlled in [13]. The switching losses can be minimized techniques were presented in [14, 15]. The input and output currents effectively regulated by prognostic current control method was introduced in [16].

## 2. DESIGN AND ANALYSIS OF LINK VOLTAGE

The resonating time is abandoned because it is greatly slighter than the power transfer time. In each of power cycle the discharging is indeterminate to takes place instead of two modes; it takes one equivalent mode in the conversion of dc-ac. The dc source is used to charging the link, with this assumption and the virtual load discharged into an equivalent value of output current for the converter operation.

Consider the above progression, the voltage across the virtual load which is equivalent to the value of output voltage can be shown as,

$$V_{0,eq} = \frac{33\sqrt{3}}{\pi} V_{0,peak} \quad (1)$$

where  $V_{0,peak}$  is the peak value of the ac-side voltage with filtered. The equivalent output current can be calculated as follows,

$$I_{0,eq} = \frac{\pi}{2\sqrt{3}} I_{0,peak} \times \cos\theta_0 \quad (2)$$

where  $\cos(\theta_0)$  and  $I_{0,peak}$  are the peak value of the ac-side power factor and ac-side current, respectively. The capacitor voltage increases linearly when the link capacitor charged by the dc-side current during the charging mode. The capacitor charged link is discharged into the virtual load during the de-energizing mode. Fig. 1 depicts that the design procedure can be carried out by the simplification of one cycle of the link voltage. Under the charging and discharging modes, the

behavior of the circuit can be described based on the following equations,

$$V_{Link,peak} = \frac{I_{dc} \times t_{charge}}{C} \tag{3}$$

$$V_{Link,peak} = \frac{I_{0,eq} \times t_{discharge}}{C} \tag{4}$$

In the aforementioned equations,  $V_{Link,peak}$ ,  $I_{dc}$ ,  $t_{discharge}$  and  $t_{charge}$  be a symbol of the peak link voltage of the capacitor, average current in the dc-side, total de-energizing time and entire energizing time during mode 1 respectively. The relationship between the discharging and charging time can be found from the Eqn. (3) and (4).

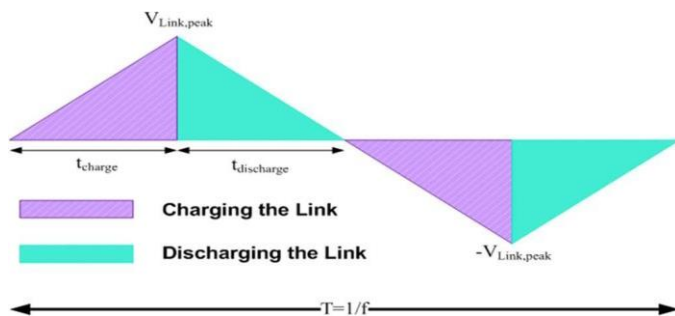


**Fig -1:** Series ac-link Inverter with one cycle of the link voltage

$$t_{charge} = \frac{I_{0,eq} \times t_{discharge}}{I_{dc}} \tag{5}$$

The average value of the voltage at dc-side can be calculated as

$$V_{dc} = \frac{1}{T} \times V_{Link,peak} \times t_{charge} \tag{6}$$

where  $T$  is the time period of the voltage at the link. From the Eqn. (5) and (6), the peak link voltage as follows,

$$V_{Link,peak} = 2V_{dc} + \frac{6\sqrt{3}}{\pi} \times V_{0,peak} \tag{7}$$

At any operating points the average value of the voltage at dc side and the amplitude of the ac-side voltage are approximately constant, then the peak voltage at link will be nearly stable over a range of power. The frequency ( $f$ ) of the link can be selected depends upon the switching characteristics and the system power rating. The link capacitance determined based upon the value of the link frequency is selected as follows,

$$C = \frac{P}{V_{Link,peak}^2 f} \tag{8}$$

From the equation, the value of link capacitor is smaller can be achieved by selecting the link frequency as higher value. The resonating periods at full power can be minimized by selecting the proper value of link inductance. The Eqn. (8) can be rewritten as,

$$f = \frac{P}{(2V_{dc} + \frac{6\sqrt{3}}{\pi} \times V_{0,peak})^2 C} \tag{9}$$

### 3. IMPLEMENTATION OF PROPOSED TECHNIQUE

The inverter proposed for the performance improvement as in Fig. 2, and this is an expansion model of the dc - dc CUK converter. The link capacitor will be charged through the side of dc and then the capacitor discharged into the side of ac during the dc-ac conversion process and the only one link to be discharged but there are three phases at the side of ac. The discharging mode will be divided into two modes by involving all three phases for lowering total harmonic distortions (THDs). The link capacitor will be charged again from the input and then discharged into the output phases during the second half cycle; but discharged and charged in reverse pathway by the link capacitor.

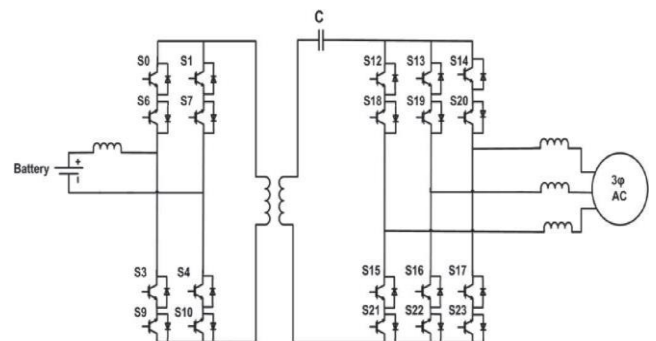


**Fig -2:** Inverter with Galvanic Isolation Method

By adding up the link with a single-phase transformer with high-frequency by provided the galvanic isolation from the series ac-link inverter. The transformer leakage inductance may play the vital role of the link inductance. Fig. 2 depicts the proposed method of inverter with galvanic isolation.

The link capacitor is charged during the side of ac and discharged into the side of dc for the period of the three-phase ac-dc conversion process. In this mode of operation have the two modes for charging and it is analogous to the conversion of

dc-ac, the both the directions of positive and negative are charged and discharged by the link, and also in between each power transfer mode a resonating mode occurs. The conversion occurs in both the directions, the link cycle has the 12 modes of operation and it consists of six resonating modes and six power transfer modes. The minimization of switching command is the significant setback during the converter operation. The incoming switches are tuned in advance of time according to that the scheme of switching was developed for the converter operations.

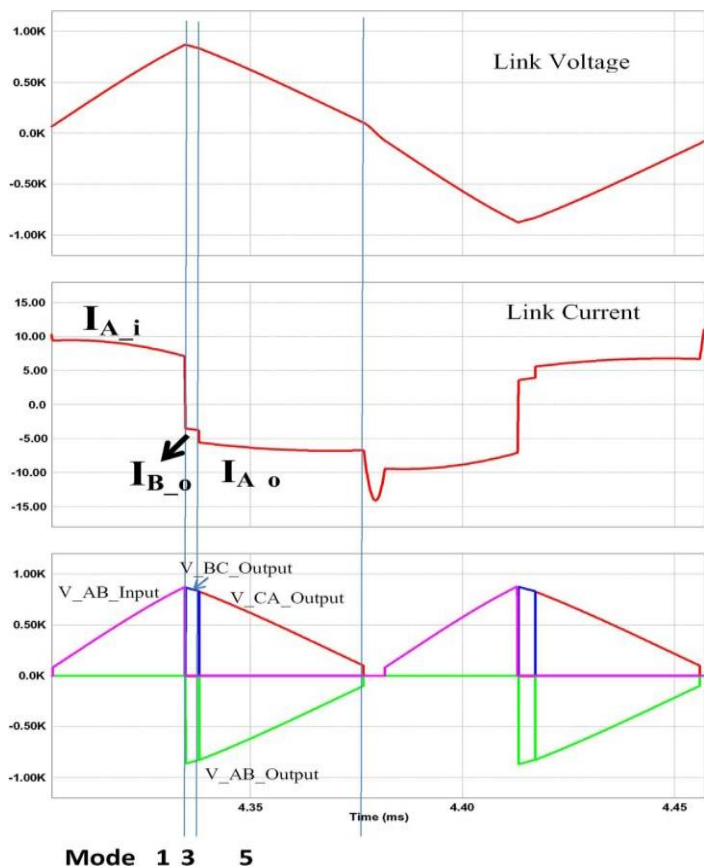


**Fig - 3:** Voltage, Current of the Link and line-to-line voltages (unfiltered) during the power conversion of dc-ac

Fig. 3 represents the behavior of the converter circuit throughout each mode and during the operation it is understandable that the phase pairs carrying the continuously maximum instantaneous value of voltage. The time span is shown in Fig. 3, it is understood that, the complete value of the current in phase A is larger than the phase B at the ac side. Fig. 3 depicts that the corresponding waveforms of ac-dc conversion. The determination of switching scheme is desired for simplifying the switching of the converters. The switches for the mode of each power transferring of conduction and during the resonating mode are identified based on zero-current turnoff and soft turn-on and minimum number of switching as well as possible in each cycle.

Fig. 4 represents the behavior of the ac-dc converter circuit throughout each mode. The polarity of the current in

the link and voltage will be decided the switches that accomplish in each power transfer mode. For example, during mode 1 operation the voltage and current at the link are positive in dc-ac converter system. The modes of main switches conducting will be based upon the line to line reference voltage and alongside with the polarities of the link current and voltage.

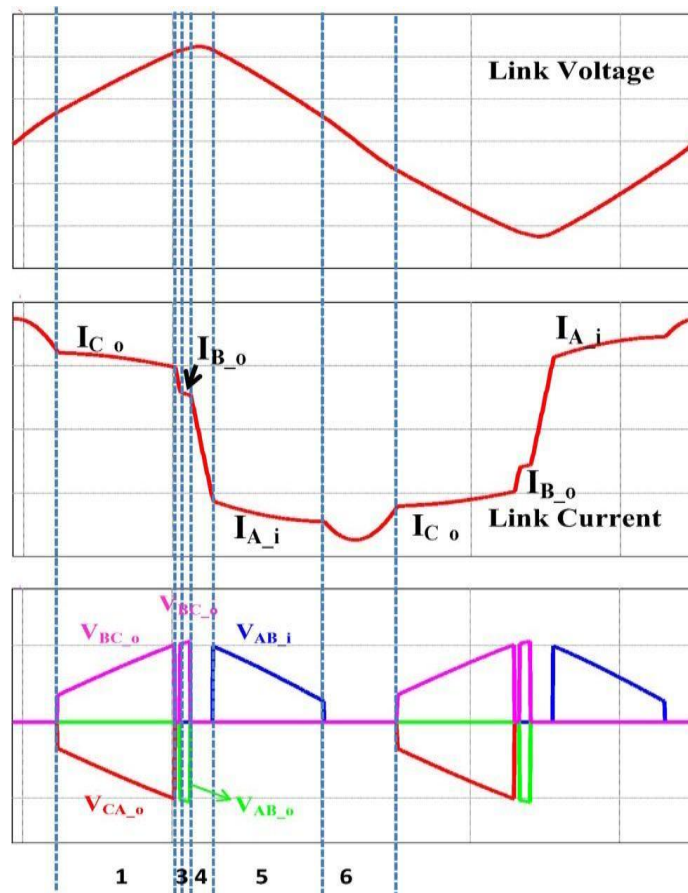


**Fig - 4:** Voltage, Current of the Link and line-to-line voltages (unfiltered) during the Power Conversion of ac-dc

#### 4. SIMULATION RESULTS AND DISCUSSIONS

The simulation results corresponding to a dc-ac converter using the proposed converter is offered. The Simulation is carried out using MATLAB. The load used for the simulation is 200-W system and input side filter of 1-mH is used. The inductor is only used to form the filter is and the harmonics are not completely attenuated and this can be completely attenuated with LCL filter. Fig. 9 shows the output current. The 2 mH of inductors each is used for output filter. The LC filter can be preferred to decrease the THD and total harmonics. The LC filter formed by a capacitor of 10μF is attached across the each load and also the neutral point. Fig. 9 shows the current at load, which has a very low THD and very smooth.



Fig - 5: Grid Side Voltage

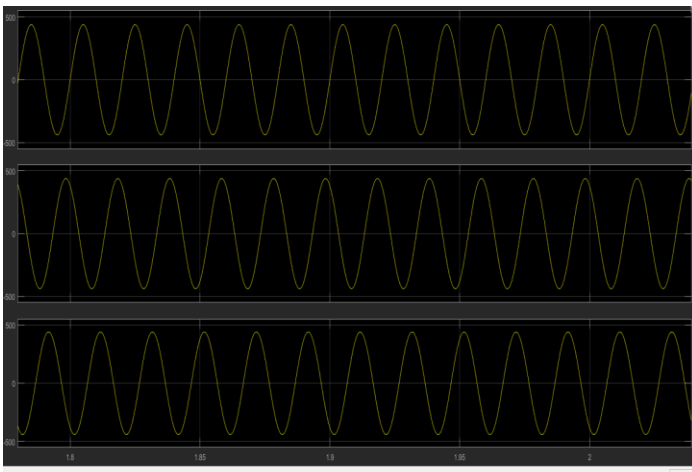


Fig - 6: Grid Side Phase to Phase Voltage

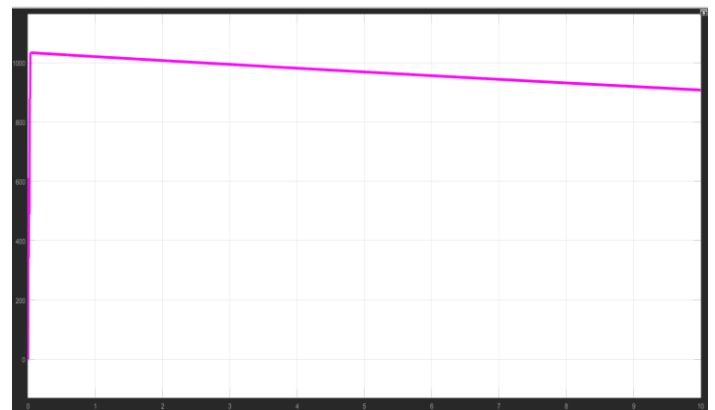


Fig - 8: Output Voltage

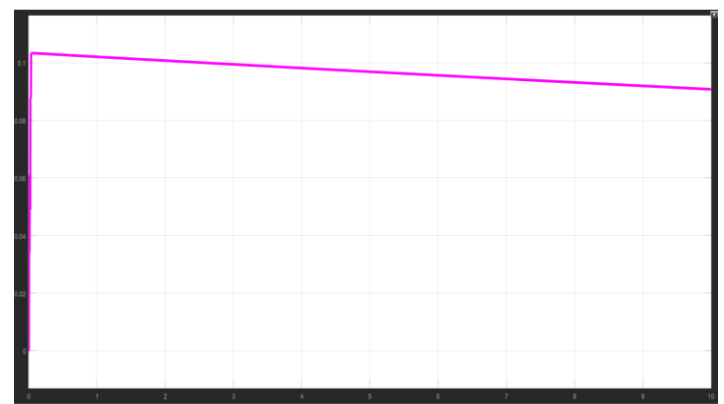


Fig - 9: Output Current

### 5. CONCLUSION

The control strategy presented is an efficient for an matrix converter of AC/DC grid voltage under the unbalanced condition to achieve sinusoidal grid current, constant voltage at output, and close to unity input power factor. The proposed control strategy provides a self-regulating control proposal for the active and reactive. By analyzing the instantaneous power in a stationary frame, the input current reference was generated sinusoidally in spite of the grid voltage under unbalanced condition. As a result, the projected technique effortlessly obtains sinusoidal grid current is synthesized directly with the reference of input current. In addition, the power factor of input becomes nearly unity by adjusting the reactive power at the grid can be zero average value. The implemented technique does not required removal of the components of grid voltage sequence or the input current controller. Subsequently the proposed scheme of control can be implemented simply without bulky storage. The efficacy of the control strategy implemented was confirmed by simulation results.

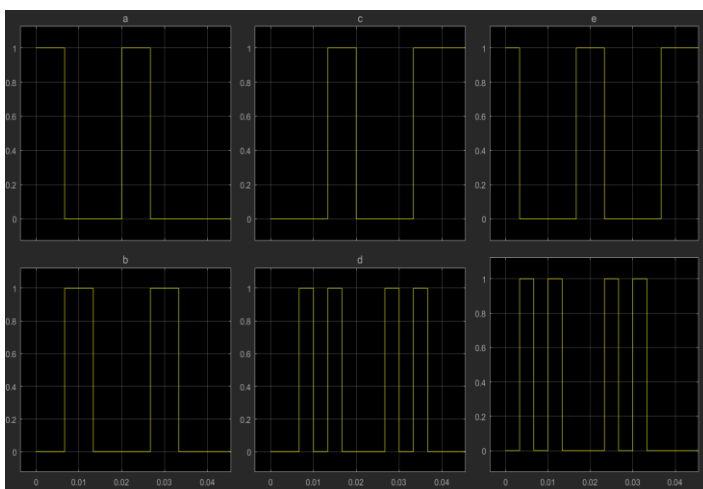


Fig - 7: Gate Pulses

**APPENDIX:**

Parameters of the Series AC link inverter:

**a) 5 KW System:**

$V_{dc}=200V$ ,  $V_{ac_{ll\_rms}} = 208V$ , Link Inductance =  $100\mu H$ , Link Capacitance =  $0.4\mu F$

**b) 200W System:**

$V_{dc}=70V$ ,  $V_{ac_{ll\_rms}} = 50V$ , Link Inductance =  $100\mu H$ , Link Capacitance =  $0.4\mu F$

**REFERENCES**

- [1] M. P. Akter, S. Mekhilef, N. M. L. Tan, and H. Akagi, "Modified Model Predictive Control of a Bidirectional AC-DC Converter Based on Lyapunov Function for Energy Storage Systems," *IEEE Trans. Ind. Electron.*, vol. 63, no.2, pp. 704–715, Feb. 2016.
- [2] P. Yang, Y. Xia, M. Yu, W. Wei, and Y. Peng, "A Decentralized Coordination Control Method for Parallel Bidirectional Power Converters in a Hybrid AC- DC Microgrid," *IEEE Trans. Ind. Electron.*, vol. 65, no. 8, pp. 6217–6228, Aug. 2018.
- [3] G. Buja, M. Bertoluzzo, and C. Fontana, "Reactive Power Compensation Capabilities of V2G-Enabled Electric Vehicles," *IEEE Trans. Power Electron.*, vol. 32, no. 12, pp. 9447–9459, Dec. 2017.
- [4] M. Yilmaz and P. T. Krein, "Review of Battery Charger Topologies, Charging Power Levels, and Infrastructure for Plug-In Electric and Hybrid Vehicles," *IEEE Trans. Power Electron.*, vol. 28, no. 5, pp. 2151–2169, May 2013.
- [5] N. M. L. Tan, T. Abe, and H. Akagi, "Design and Performance of a Bidirectional Isolated DC-DC Converter for a Battery Energy Storage System," *IEEE Trans. Power Electron.*, vol. 27, no. 3, pp. 1237–1248, Mar. 2012.
- [6] M. A. Sayed, K. Suzuki, T. Takeshita, and W. Kitagawa, "PWM Switching Technique for Three-Phase Bidirectional Grid-Tie DC-AC- AC Converter With High-Frequency Isolation," *IEEE Trans. Power Electron.*, vol. 33, no. 1, pp. 845–858, Jan. 2018.
- [7] D. Varajão, R. E. Araújo, L. M. Miranda, and J. A. P. Lopes, "Modulation Strategy for a Single-Stage Bidirectional and Isolated AC- DC Matrix Converter for Energy Storage Systems," *IEEE Trans. Ind. Electron.*, vol. 65, no. 4, pp. 3458–3468, Apr. 2018.
- [8] H. N. Nguyen and H. H. Lee, "An Effective SVM Method for Matrix Converters With a Superior Output Performance," *IEEE Trans. Ind. Electron.*, vol. 65, no. 9, pp. 6948–6958, Sep. 2018.
- [9] G. Rizzoli et al., "Comparison between an AC-DC matrix converter and an interleaved DC-dc converter with power factor corrector for plug-in electric vehicles," in *2014 IEEE International Electric Vehicle Conference (IEVC)*, 2014, pp. 1–6.
- [10] M. Su, H. Wang, Y. Sun, J. Yang, W. Xiong, and Y. Liu, "AC/DC Matrix Converter With an Optimized Modulation Strategy for V2G Applications," *IEEE Trans. Power Electron.*, vol. 28, no. 12, pp. 5736– 5745, Dec. 2013.
- [11] B. Feng, H. Lin, and X. Wang, "Modulation and control of ac/dc matrix converter for battery energy storage application," *IET Power Electron.*, vol. 8, no. 9, pp. 1583–1594, 2015.
- [12] S. Liu, Xiao; Zhang, Qingfan; Hou, Dianli; Wang, "Improved Space Vector Modulation Strategy for AC-DC Matrix Converters," *J. Power Electron.*, vol. 13, no. 4, pp. 647–655, 2013.
- [13] K. You, D. Xiao, M. F. Rahman, and M. N. Uddin, "Applying Reduced General Direct Space Vector Modulation Approach of AC-AC Matrix Converter Theory to Achieve Direct Power Factor Controlled ThreePhase AC- DC Matrix Rectifier," *IEEE Trans. Ind. Appl.*, vol. 50, no. 3, pp. 2243–2257, May 2014.
- [14] M. Mengoni, L. Zarri, A. Tani, G. Rini, G. Serra, and D. Casadei, "Modulation strategy with minimum switching losses for three-phase AC-DC matrix converters," in *2014 16th European Conference on Power Electronics and Applications*, 2014, pp. 1–10.
- [15] M. Mengoni, L. Zarri, A. Tani, G. Rizzoli, G. Serra, and D. Casadei, "Modulation strategies for three-phase AC-DC matrix converters: A comparison," in *2016 IEEE Energy Conversion Congress and Exposition (ECCE)*, 2016, pp. 1–7.
- [16] B. Feng and H. Lin, "Finite Control Set Model Predictive Control of AC/DC Matrix Converter for Grid-Connected Battery Energy Storage Application," *J. Power Electron.*, vol. 15, no. 4, pp. 1006–1017, 2015.